# STUDY ON THERMAL INSULATION OF LIQUEFIED NATURAL GAS CRYOGENIC ROAD TANKER

by

***Edward LISOWSKI***[a] ***and Filip LISOWSKI***[b*]

[a]Institute of Applied Informatics, Cracow University of Technology, Cracow, Poland
[b]Institute of Machine Design, Cracow University of Technology, Cracow, Poland

Original scientific paper
https://doi.org/10.2298/TSCI19S4381L

*The tanks designed for liquefied natural gas transport must be thermally insulated from the environment due to the low condensing temperature of the gas. The effectiveness of thermal insulation significantly affects the tank's operating parameters and its operating costs. As there is no perfect insulation, there is a need for analyses that would determine its suitability in specific applications. In this paper the issue of heat transfer through double-walled cryogenic tanks with evacuated insulation system was discussed. Afterwards the study of insulation variants of liquefied natural gas cryogenic road tanker was presented. The use of several layers of insulation made of modern and efficient materials such as aerogel and fiberglass or the use of multi-layer isolation has been considered and compared to the use of perlite powder. The heat flux through insulation systems was tested for different variants of evacuated insulation under residual gas pressure of $10^{-1}$ Pa, $10^{-3}$ Pa, and 100 kPa. Finally, for selected insulation variants, the heat leakage was tested for 50 $m^3$ liquefied natural gas road tanker. The investigation of heat-flow for the transient thermal analysis was performed by applying finite element method. The aim of the study was to determine the variant of insulation system with the relatively low heat leakage to the tank and low cost of materials and vacuum production.*

Key words: *liquefied natural gas, thermal insulation, road tanker*

## Introduction

The increase in the importance of liquefied natural gas (LNG) in recent years is related to the general increase in the demand for natural gas. It is relatively cheap fuel with high ecological value. As a result of LNG condensation, gas volume decreases more than 600 times. The liquefaction of natural gas is associated with its very thorough purification of $CO_2$, nitrogen, propane-butane, *etc*. In addition, after the LNG is changed from the liquid state to the gaseous state, it is free of impurities and moisture. Due to the low condensing temperature, for storage and transport of LNG, quite complicated cryogenic tanks are required.

The cryogenic road tankers are typically designed as double-walled tanks with evacuated annular space, fully or partially filled by insulation material. An internal vessel and ex-

* Corresponding author, e-mail: Filip.Lisowski@mech.pk.edu.pl

ternal jacket are usually made of austenitic stainless steels, which contain more than 7% of nickel and remain ductile down to low temperatures [1]. The inner tank is installed on internal supports, which construction should provide low heat transfer and proper mechanical strength. Since no cooling systems are used, it is necessary to use appropriate insulation. The insulation systems of such tanks can vary in vacuum pressure as well as the amount and type of insulating materials.

Thermal insulation plays significant role in cryogenic tanks. It provides the stable parameters of the tank operation in the range of design temperatures and protects against adverse effects of sudden loss of vacuum. The effectiveness of thermal insulation depends on gas pressure known as the cold vacuum pressure (CVP), applied materials and their configuration.

The choice of insulation system primarily depends on required vacuum level and therefore on dominant mechanisms of heat transfer: radiation, gas conduction, and convection. Depending on its application in cryogenic system, there are three categories of vacuum: high vacuum (HV) for pressure from $1.33 \cdot 10^{-4}$ to $1.33 \cdot 10^{-1}$ Pa, soft vacuum (SV) from 1.33 to 1333 Pa, and no vacuum (NV) from 13.3 to 133 kPa [2].

The vacuum pressure is the first design parameter that affects costs in most applications. The second parameter is the total mass of installed insulation that is often critical for transportation application. Bearing in mind that the permissible axle loads are specified, it is easy to notice that the lower the weight of the insulation system the more cargo can be transported. Durability and resistance to variable thermal and mechanical loads are also crucial for cryogenic road tanker design.

Despite the numerous publications quoted below, which deal with the types and thermal parameters of vacuum insulation systems for application in cryogenic tanks, none of them undertakes the analysis related directly to the application in a road tanker. In this article, the performance of various vacuum insulation systems has been numerically tested to determine whether they are appropriate for use in road tankers.

## Insulation systems for LNG cryogenic road tankers

In general, insulation materials for cryogenic applications can be divided into three groups: foams, bulk-fill and layered [3].

The foam insulation materials offer thermal conductivity in the range of 35-55 mW/(mK) [4] and require NV. Typical foam insulations include polyurathene or polystyrene foam. Effectiveness of rigid foam insulations can degrade dramatically over time and the high thermal expansion of the foams causes a tendency to crack at low temperatures or under cyclic load [5]. For safety reasons, insulation materials should be also incombustible and self-extinguishing [6]. Although tanks with expanded polyurathene foam insulations were produced, those foams do not meet the previous requirements and it is not favorable for application in mobile tanks. Therefore, bulk-fill and layered insulation systems are most often considered for use in mobile tanks design.

The bulk-fill powders insulations have been mainly used in stationary or large transportation containers. The best known microporous material is an expanded perlite with bulk density from 50-300 kg/m$^3$ [7]. This cheap, natural origin material has thermal conductivity coefficient 1-2 mW/(mK) under vacuum pressure around 0.1 Pa. [3]. Other well-known powders are: glass bubbles, silica aerogels, or composites. The glass bubbles have a slightly lower heat conduction coefficient than perlite or aerogel powders. In turn, aerogel powders with microporous cellular structure has high compressive strength, but at high production costs [7]. However, the powder materials have the tendency to settle and compact due to vibration and thermal cycling loads. It leads to degradation of thermal properties and can cause damages [1].

The best thermal performance, as low as 0.03 mW/(mK), can be obtained in the laboratory conditions for multi-layer insulation (MLI) [2]. The MLI, also known as superinsulation, requires vacuum level below $10^{-3}$ Pa to be fully effective [8]. It consists of a large number of highly reflecting shields separated by spacers having low conductivity. When the pressure distribution is very homogeneous, the local thermal conductivity between the radiation shields is strongly suppressed [9]. The MLI is sensitive to mechanical compression and edge effects. The effectiveness of MLI depends on vacuum level. In case of sudden loss of vacuum, thermal performance can degrade rapidly causing a dangerous pressure increase inside the inner tank [10]. Furthermore, the steps of evacuation, heating, and vacuum retention are expensive and time consuming [1].

The other layered insulation systems that incorporate aerogel or fiberglass composite blankets can remain effective even at SV level [11]. In that case the conduction is greater and those systems will not be as efficient as MLI at HV level.

The aerogels are flexible, highly porous materials, which have low density and high porosity that makes them very good insulators. However, compressive loads may affect the thermal resistance due to their structure [12].

In comparison to MLI and powder materials, based on experimental studies, the best performance for SV and NV ranges was obtained for aerogel composite blanket [2].

Another material, developed as an alternative to commonly used perlite is the micro-fiberglass material Cryo-Lite®. Its low density minimizes tanker weight, eliminates problem with settling or compaction and offers fast vacuum pump down rates with minimal outgassing [8]. Due to its low opacity Cryo-Lite® blankets should be used with radiation shields to reduce radiation heat transfer.

Since the effectiveness of MLI is about 50% worse at atmospheric pressure, system involving combination of MLI and aerogels [13] or MLI and fiberglass blankets were also tested [8]. Experimental results showed that combination of different insulation materials can improve insulation system effectiveness and it was found that it is significant whether a particular material is placed on the warm or cold side.

The use of vacuum insulation systems for application at 50 m$^3$ LNG truck tanker containing expanded perlite, silica aerogel blanket Cryogel Z®, fiberglass blanket Cryo-Lite®, and MLI system were studied.

## Heat ransfer to the tank

There are three mechanisms of heat transfer that can occur in cryogenic tanks with vacuum insulation system. Those are: conduction, convection, and radiation.

### *Conduction in solids*

The heat transfer by conduction occurs in tank's walls, pipes, supports and other elements connected to the tank. For LNG tanker the difference between liquid and environment can be around 200 K. In that case, the heat conduction can be considered as 1-D problem under steady-state conditions [3] described by Fourier's equation:

$$\dot{q} = k\text{grad}(T) \tag{1}$$

### *Conduction in residual gas*

There are two heat transfer regimes depending on the ratio between free path of the gas molecules $\lambda$ and the distance $l$ between tank walls. For $\lambda \gg l$ the free molecular regime is applied, whereas for $\lambda \ll l$ the hydrodynamic regime is valid. Molecular regime is obtained at low gas pressure. In that case heat transfer depends on the residual gas pressure and is independent from distance, $l$. The rate of heat transfer in the free molecular regime is described by Kennard's law [14]:

$$\dot{Q} = A\alpha_r \left(\frac{\gamma+1}{\gamma-1}\right)\sqrt{\frac{\bar{\mathrm{R}}}{8\pi\bar{M}}}\frac{T}{\sqrt{T}}p \quad \text{where} \quad \gamma = \frac{c_p}{c_v} \tag{2}$$

### *Convection*

Convection in LNG tanker under cryogenic condition does not differ from convection in higher temperatures. When there is an interaction with solid surface, the heat transferred from the liquid gas to the tank wall is modeled by Newton's law [7]:

$$\dot{q} = \alpha\left(T_s - T_l\right) \tag{3}$$

Using the eq. (3) requires the value of heat transfer coefficient, $\alpha$, which usually must be determined experimentally as a function of temperature.

### *Radiation*

Heat radiation is a process that occurs in each body with temperature higher than absolute zero. The heat flux transmitted by heat radiation between two bodies with temperatures $T_1$ and $T_2$, wherein $T_1 > T_2$, can be determined using the equation [3]:

$$\dot{q} = \sigma\varepsilon\left(T_1^4 - T_2^4\right) \tag{4}$$

The heat radiation between two surfaces can be reduced by applying radiation shields made of material with low emissivity. Increasing the number of radiation shields improves efficiency of the insulation.

## **Modelling of the heat transfer through tank insulation**

In order to verify usability of several insulating materials for application in LNG cryogenic road tanker, heat transfer through different evacuated insulation systems and temperature distribution were examined by applying transient thermal analysis using ANSYS software. The 2-D models within cross-section of the tank walls and insulation system, analogous as shown in the fig. 1 were accepted. The study included four different insulation materials in several variants as given in tab. 1. Each variant was tested in three levels of the residual gas pressure: $10^{-1}$ Pa, $10^{-3}$ Pa, and 100 kPa.

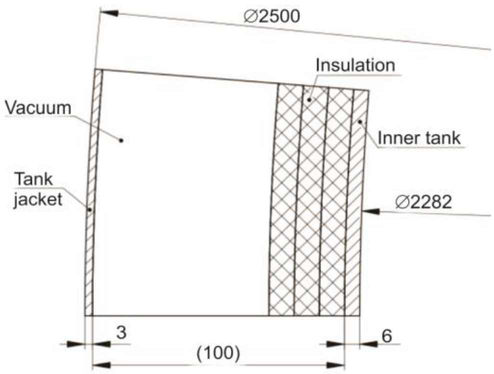

**Figure 1. The 2-D model of the exemplary insulation system**

### *Material properties and assumptions for numerical analysis*

Mechanical and thermal properties of steels as well as properties of insulation materi-

**Table 1. Variants of the tested insulation systems**

| Insulation material | Number of layers | Insulation thickness, [mm] |
|---|---|---|
| Cryogel® Z | 2 | 20 |
| Cryogel® Z | 4 | 40 |
| Cryogel® Z | 6 | 60 |
| Cryogel® Z | 8 | 80 |
| Cryogel® Z | 10 | 100 |
| Cryo-Lite® | 1 | 25 |
| Cryo-Lite® | 2 | 50 |
| Cryo-Lite® | 3 | 75 |
| Cryo-Lite® | 5 | 100 |
| MLI | 40 | 16 |
| Perlite | – | 100 |

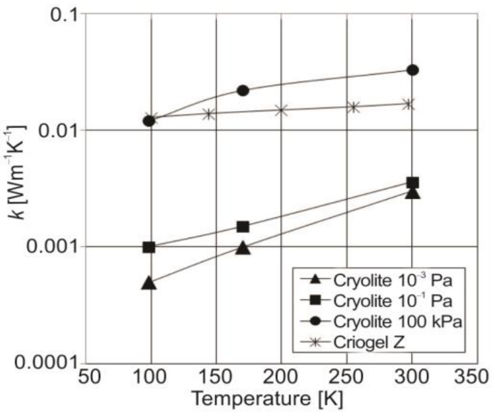


**Figure 2. Thermal conductivity of Cryo-Lite® and Cryogel® Z (vendor data)**

als and residual gas depend on pressure and temperature. A stainless steel 1.4301 was accepted as a material of inner vessel and outer jacket. The coefficient of thermal conductivity in the function of temperature for insulating materials such as Cryo-Lite® and Cryogel® Z in the fig. 2, whereas for steel 1.4301 is shown in fig. 3. The MLI insulation consisted of 40 layers of double-aluminized Mylar and polyester net spacer. An expanded perlite involved in analysis has bulk density 200 kg/m$^3$. The coefficients of thermal conductivity in the function of pressure for MLI and perlite are given in tab. 2. Accepted values were obtained at Cryostat-100 test at boundary temperatures 77 and 273 K [2].

**Table 2. Coefficients of thermal conductivity for MLI and perlite [2]**

| Material | $k$ [Wm$^{-1}$K$^{-1}$] | CVP [Pa] |
|---|---|---|
| MLI | 0.028 | $10^{-3}$ |
| MLI | 0.072 | $10^{-1}$ |
| MLI | 35 | $10^{5}$ |
| Perlite | 0.95 | $10^{-3}$ |
| Perlite | 1 | $10^{-1}$ |
| Perlite | 44 | $10^{5}$ |

Coefficient of thermal conductivity of residual gas under pressure of $10^{-1}$ Pa was assumed equal to 0.01 W/mK [4]. For the case of NV, the assumed gas pressure of 100 kPa corresponds to atmospheric pressure. Coefficient of thermal conductivity in the function of temperature for dry air was accepted as presented in the fig. 4.

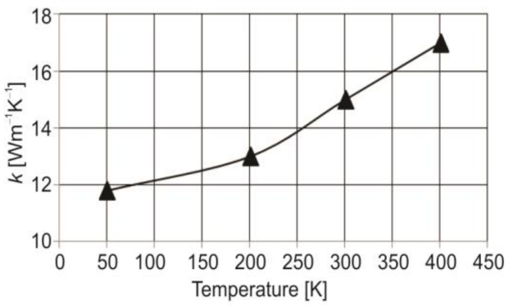


**Figure 3.Thermal conductivity of stainless steel 1.4301 [15]**

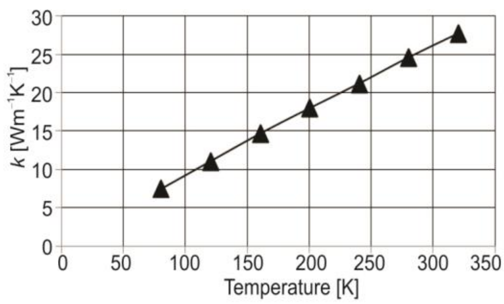


**Figure 4. Thermal conductivity of dry air at 100kPa [16]**

The following assumptions were made for numerical analysis:

– the model is in a state of thermal equilibrium, which is obtained after 24 hours,

– the internal surface of inner tank exchanges heat with liquid by convection with accepted convection coefficient 337 W/m$^2$K at 77 K [17],
– the external surface of tank jacket exchanges heat with environment by convection with accepted convection coefficient 8.89 W/m$^2$K at 293 K [17],
– heat is transferred through insulation layers only by conduction with accepted coefficient of thermal conductivity,
– for residual gas pressure of $10^{-1}$ Pa and 100 kPa, heat is transferred by conduction and by radiation,
– for residual gas pressure of $10^{-3}$ Pa, heat is transferred through residual gas only by radiation,
– for layered insulation systems, external layer of insulation is covered with an aluminum radiation shield with emissivity $\varepsilon = 0.03$ [16],
– surface to surface model of radiation was accepted, and
– the mesh was validated based on global refinement, the coarse mesh has been refined until difference in average heat flux between following steps was less than 3%

### *Simulation results*

The comparative results of the transient thermal analysis are presented in diagrams as well as in the maps of heat flux and temperature distribution. Figure 5 shows the exemplary

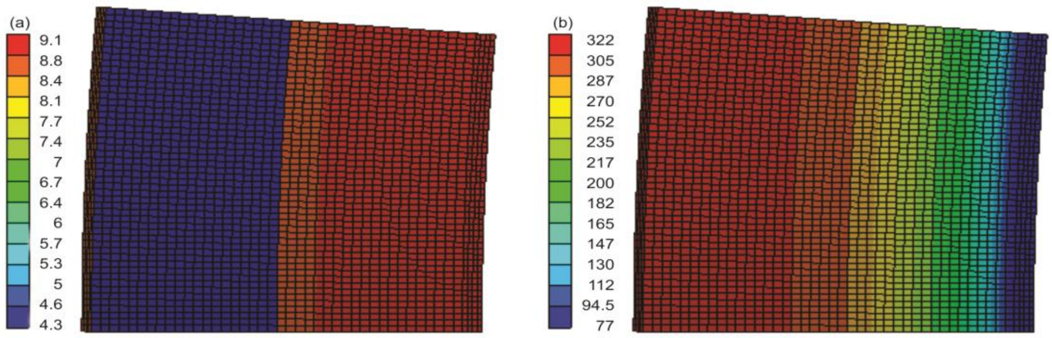


**Figure 5. (a) Heat flux [Wm$^{-2}$], (b) temperature [K] for the cross-section of insulation system with Cryo-Lite® under $10^{-1}$Pa**

results of heat flux and temperature distribution in the cross-section of insulation system involving Cryo-Lite® under vacuum pressure of 10¯1 Pa. Figures 6 and 7 summarize average heat flux in the cross-section of the inner tank wall for insulation systems containing Cryo-Lite® and Cryogel® insulation blankets. Figure 8 presents results for insulation systems including MLI, perlite and only residual gas.

Due to relatively small wall thickness of the tank jacket usually accepted in tanker design, the tank jacket must have stiffening ribs on the inside. Assuming that the maximum height of the ribs is 40 mm, insulation variants with a thickness less than or equal to 60 mm have been selected for further analysis on heat leakage, product loss and storage time for 50 m$^3$ LNG cryogenic road tanker.

## Testing of the heat leakage, product loss, and storage time

### *Calculation methodology*

The heat leakage, product loss and storage time were tested for 50 m$^3$ LNG road tanker for four variants of selected insulation systems as given in tab. 3. The methodology

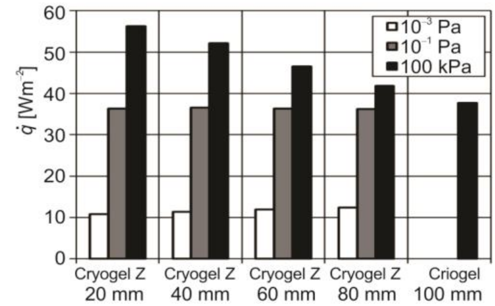


**Figure 6. Average heat flux in the cross-section of inner tank wall for insulation system with Cryogel® Z**

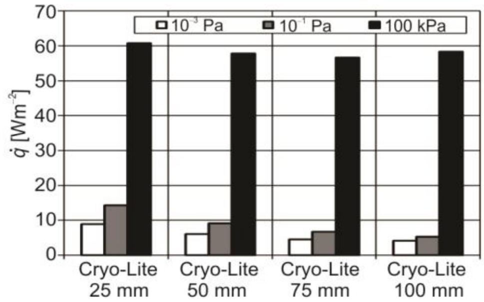


**Figure 7. Average heat flux in the cross-section of inner tank wall for insulation system with Cryo-Lite®**

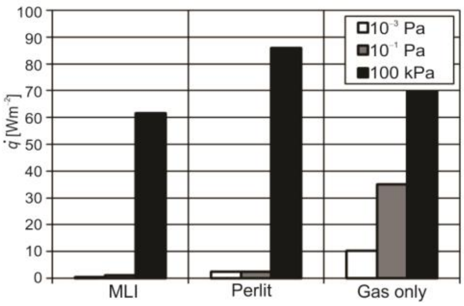


**Figure 8. Average heat flux in the cross-section of inner tank wall for insulation systems with MLI, perlite, and gas only**

presented in the EN 12213 [18] was used. The heat leakage is a ratio of the product loss and latent heat of evaporation, eq. (5). Whereas the product loss, $L$ [%], of mass per day is given by eq. (6). The storage time in days is equal to 100/L:

$$\dot{Q}_c = h_{fg}\dot{m} \tag{5}$$

$$L = \frac{86400\dot{Q}A}{h_{fg}F} \tag{6}$$

Latent heat of LNG evaporation $5.1\cdot10^5$ J/kg was accepted. The heat leakage to the tank was accepted to be equal to the heat on the outer surface of the tank jacket obtained on the basis of transient thermal analysis using finite element method.

**Table 3.Variants of the tested insulation systems**

| Insulation material | Number of layers | Insulation thickness, [mm] |
|---|---|---|
| Cryogel® Z | 6 | 60 |
| Cryo-Lite® | 2 | 50 |
| MLI | 40 | 16 |
| Perlite | – | 100 |

### *Geometry and assumptions*

The finite element analysis included modeling of heat transfer through insulation system and residual gas as well as through internal supports. A system of polyamide internal supports proposed by Lisowski *et. al* [19] was accepted. The heat leakage through piping was omitted in the study. The dimensions of considered tanker are summarized in the tab. 4.

**Table 4. Dimensions of 50 m$^3$ LNG road tanker**

| Name | Dimension |
|---|---|
| Outer diameter of the inner tank | 2300 mm |
| Outer diameter of the tank jacket | 2500 mm |
| Wall thickness of the inner tank | 5 mm |
| Wall thickness of the tank jacket | 3 mm |
| Insulation thickness | 16-100 mm |
| Cross-sectional area of one support | 0.04 m$^2$ |
| Cross-sectional area of all supports | 1.44 m$^2$ |

In comparison to previous analysis of insulation systems on the basis of 2-D models, the additional assumptions were made:

- the internal surface of inner tank exchanges heat with liquid by convection with accepted convection coefficient at 110 K,
- the external surface of tank jacket exchanges heat with environment by convection with accepted convection coefficient at 323 K,
- heat is transferred through polyamide supports by conduction with accepted coefficient of thermal conductivity according to fig. 9, and
- between polyamide supports, inner tank and tank jacket, thermal contact resistance was defined with respectively accepted thermal contact coefficients 0.3 and 50 m$^2$K/W [15].

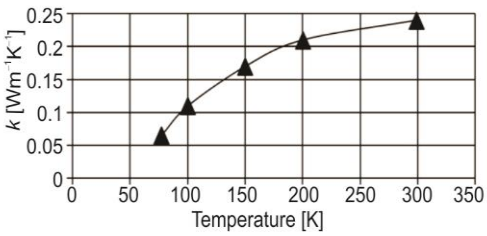


**Figure 9. Thermal conductivity of polyamide PA6 [19]**

*Tests results*

The exemplary results of heat flux and temperature distribution for 50 m$^3$ LNG road tanker with insulation system involving Cryo-Lite® and vacuum pressure of 10$^{-1}$Pa are shown in the figs. 10 and 11. The average heat rate on the outer surface of the tank jacket obtained from the transient thermal analysis is summarized in the fig. 12. The resulted values of equivalent product loss per day and storage time are presented in the figs. 13 and 14.

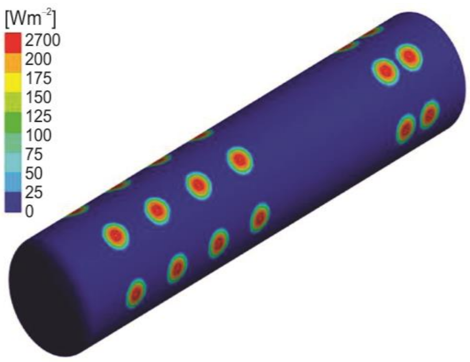


**Figure 10. Heat flux distribution for 50 m$^3$ LNG road tanker with Cryo-Lite® under 10-1Pa**


**Figure 11. Temperature distribution for 50 m$^3$ LNG road tanker with Cryo-Lite® under 10-1Pa**

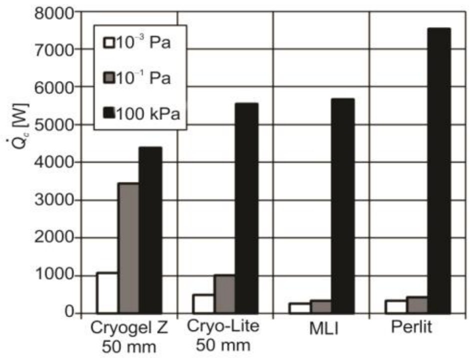


**Figure 12. The heat leakage to 50 m$^3$ LNG road tanker for different insulation systems**

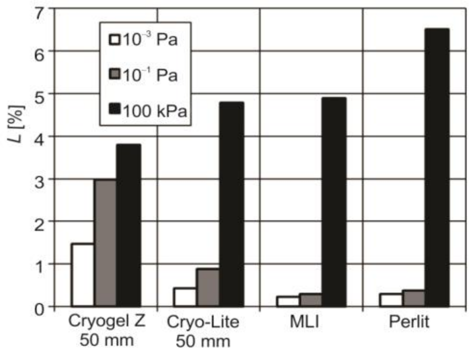


**Figure 13. Equivalent product loss per day for 50 m$^3$ LNG road tanker for different insulation systems**

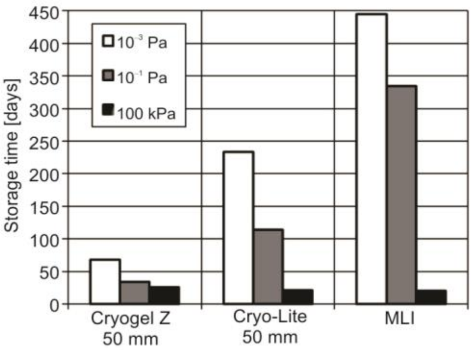


**Figure 14. Storage time for different insulation systems of 50 m$^3$ LNG road tanker**

## Results and discussion

The results of thermal analysis of 2-D models show that for insulation system with Cryogel®Z, in the case of vacuum loss, the insulation thickness has a significant impact on the heat leakage. Depending on the thickness of insulation, the calculated heat flux was 38-56 W/m$^2$. For SV or HV range, the average heat flux was constant regardless of the number of insulation layers. The average heat flux obtained from simulation was about 37 W/m$^2$ for SV and about 12 W/m$^2$ for HV.

For insulation system with Cryo-Lite®, the impact of insulation thickness is much smaller in the case of vacuum loss. The average heat flux through insulation system obtained for that case was around 60 W/m$^2$ independent on the insulation thickness. In turn, for the SV and HV range, the average heat flux depends on number of insulation layers. The average heat flux obtained from simulation was in the range of 5-14 W/m$^2$ for SV and about 4-9 W/m$^2$ for HV depending on number of insulation layers.

For insulation system with MLI, in the case of vacuum loss, the average heat flux through insulation system was around 60 W/m$^2$, whereas for insulation system with perlite it was higher and reached 85 W/m$^2$. However, for the soft and HV range, these two insulation systems have the lowest heat leakage to the tank. It was respectively 1.2 W/m$^2$ for MLI and 2.6 W/m$^2$ for perlite in the SV range and 0.4 W/m$^2$ for MLI and 2.4 W/m$^2$ for perlite in the HV range.

The results of storage time calculations for 50 $m^3$ LNG road tanker show that using MLI insulation system, for HV pressure of $10^{-3}$ Pa, provide the longest storage time, close to 450 days. The result for SV pressure of $10^{-1}$ Pa was around 330 days.

Satisfactory results were also obtained for applying Cryo-Lite® fiberglass blankets. The storage time for HV range was about 230 days, whereas for SV range was about 115 days. This period seems to be long enough for application in cryogenic LNG road tankers. It also should be noted that for non-vacuum range of residual gas, in comparison to the other materials, slightly longer storage time was obtained for insulation system with Cryogel® blankets.

## Conclusions

Thermal insulation plays an important role in the construction of cryogenic tanks. Its effectiveness depends on applied materials and vacuum pressure. The thermal performance of cryogenic road tankers have to be considered in reference to the whole structure and include the analysis of the heat leakage through internal supports, piping and other thermal bridges.

The results of simulations show that MLI system in comparison with other tested cryogenic insulation systems is the best performer in the HV range of residual gas pressure of $10^{-3}$ Pa and SV range of $10^{-1}$ Pa. Bulk-fill expanded perlite is the second, followed by the fiberglass and aerogel blankets. Cryogel®Z aerogel insulation blanket turned out to be the best performer in the range of NV at pressure of 100 kPa.

For analysis of the entire tank with internal supports, the insulation system with two layers of Cryo-Lite® fiberglass blankets had slightly worse thermal performance than insulation systems with MLI and perlite, but it was better in case of vacuum loss. Apart from good insulation properties due to the tendency to settle and compact under the influence of vibration, the perlite insulation system seems not to be the best solution for road tanker applications. However, as the analyses have shown, it can be successfully replaced by MLI or Cryo-Lite®.

It was also verified that the range of vacuum pressure in the insulation system is a significant parameter that affects the storage time. Due to the product loss caused by evaporation of LNG, for 50 $m^3$ LNG cryogenic road tanker it is necessary to apply soft or HV range with thermal insulation system.

## Nomenclature

$A$ – area of the outer surface of the tank, [$m^2$]
$c_p$ – specific heat at constant pressure, [$Jkg^{-1}K^{-1}$]
$c_v$ – specific heat at constant volume, [$Jkg^{-1}K^{-1}$]
$F$ – total mass of LNG in the tank, [kg]
$h$ – heat transfer coefficient, [$Wm^{-2}K^{-1}$]
$h_{fg}$ – latent heat of vaporization, [$Jkg^{-1}$]
$k$ – thermal conductivity, [$Wm^{-2}K^{-1}$]
$L$ – equivalent product loss per day, [–]
$l$ – distance between surfaces exchanging heat, [m]
$\bar{M}$ – molar mass, [$kgmol^{-1}$]
$\dot{m}$ – actual flux of product loss, [$kgs^{-1}$].
$p$ – pressure, [Pa]
$\bar{R}$ – universal gas constant, [$Jmol^{-1}K^{-1}$]
$T$ – temperature, [K]
$T_s$ – temperature of solid, [K]
$T_l$ – temperature of liquid, [K]
$\dot{Q}$ – heat leakage [W]

*Greek symbols*

$\alpha_r$ – overall accommodation coefficient, [–]
$\varepsilon$ – emissivity, [–]
$\lambda$ – free path of the gas molecules, [–]
$\sigma$ – Stefan-Boltzmann constant, [$Wm^{-2}K^{-4}$]

## References

[1] Augustynowicz, S. D., *et al*., Cryogenic Insulation Systems, *Proceedings*, 20th International Congress of Refrigeration, Sydney, Australia, 1999
[2] Fesmire, J. E., Standardization in Cryogenic Insulation Systems Testing and Performance Data, *Physics Procedia, 67* (2015), Dec., pp. 1089-1097

[3] Flynn, T. M., *Cryogenic Engineering*, Second Edition, Marcell Dekker, New York, USA, 2005
[4] Chorowski, M., *Cryogenics Fundamentals and Applications* (in Polish), IPPU Masta, Gdansk, Poland, 2005
[5] Bahadori, A., Thermal Insulation Handbook for Oil, Gas and Petrochemical Industries, Elsevier, Amsterdam, The Netherland, 2014
[6] Planas-Cuchi, E., *et al*., Explosion of a Road Tanker Containing Liquefied Natural Gas, *Journal of Loss Prevention in the Process Industries, 17* (2004), 4, pp. 315-321
[7] Bunger, U., Owren, G., Development Potentials for Small Mobile Tanks with Vacuum Powder Insulations, *International Journal of Hydrogen Energy, 23* (1998), 4, pp. 273-279
[8] Kogan, A., *et al*., Cryogenic Vacuum Insulation for Vessels and Piping, NASA Technical Report, Nr. KSC-2010-126
[9] Reiss, H., A Coupled Numerical Analysis of Shield Temperatures, Heat Losses and Residual Gas Pressures in an Evacuated Super-Insulation Using Thermal and Fluid Networks Part I: Stationary Conditions, *Cryogenics, 44* (2004), 4, pp. 259-271
[10] Xie, G. F., *et al*., Study on the Heat Transfer of High-Vacuum- Muli-Layer-Insulation Tank After Sudden, Catastrophic Loss of Insulating Vacuum, *Cryogenics, 50*, (2010), 10, pp. 682-687
[11] Coffman, B. E., *et al*., Aerogel Blanketinsulation Materials for Cryogenic Applications, *Advances in Cryogenics Engineering AIP Conf. Proc. 1218, 913* (2010), 1, pp. 913-920
[12] Hoseini, A., *et al*., Deformation And Thermal Resistance Study of Aerogel Blanket Insulation Material Under Unaxial Compression, *Energy and Buildings, 130* (2016), Aug., pp. 228-237
[13] Johnson, W. L., *et al*., Analysis and Testing of Muli-Layer and Aerogel Insulation Configurations, *Advances in Cryogenics Engineering AIP Conf. Proc. 1218, 913* (2010), 1, pp. 780-787
[14] Baudouy, B., Heat Transfer and Cooling Techniques at Low Temperature, CERN Yellow Report CERN-2014-005, pp.329-352
[15] Czyzycki, W., Heat Flow Modelling on Thermal Insulation of Cryogenics Tanks using SolidWorks Simulation package, Technical Transactions, Mechanics, 4-M/2011, 7, pp. 29-36
[16] Vargaftik, N. B., *et al*., *Handbook of Thermal Conductivity of Liquids and Gases*, CRC Press, Boka Raton, Fla., USA, 2005
[17] Czyzycki, W., Modeling of Heat Flow through Muli-Layer Internal Supports of Cryogenic Vessels, Technical Transactions, Mechanics, 2-M/2015, pp. 27-34
[18] ***, EN 12213:2001, Cryogenic Vessels. Methods for Performance Evaluation of Thermal Insulation
[19] Lisowski, E., *et al*., 2010, Using of Polyamide in Construction of Supporting Blocks of Cryogenic Tanks on Example of LNG Container, *Archives of Foundry Engineering, 10* (2100), Special Issue 3, pp. 81-86

Paper submitted: March 12, 2019
Paper revised: April 29, 2019
Paper accepted: May 20, 2019